UCRL -9647

UNIVERSITY OF CALIFORNIA

Ernest O. Lawrence Radiation Laboratory

TWO-WEEK LOAN COPY

This is a Library Circulating Copy which may be borrowed for two weeks. For a personal retention copy, call Tech. Info. Division, Ext. 5545

BERKELEY, CALIFORNIA

DISCLAIMER

This document was prepared as an account of work sponsored by the United States Government. While this document is believed to contain correct information, neither the United States Government nor any agency thereof, nor the Regents of the University of California, nor any of their employees, makes any warranty, express or implied, or assumes any legal responsibility for the accuracy, completeness, or usefulness of any information, apparatus, product, or process disclosed, or represents that its use would not infringe privately owned rights. Reference herein to any specific commercial product, process, or service by its trade name, trademark, manufacturer, or otherwise, does not necessarily constitute or imply its endorsement, recommendation, or favoring by the United States Government or any agency thereof, or the Regents of the University of California. The views and opinions of authors expressed herein do not necessarily state or reflect those of the United States Government or any agency thereof or the Regents of the University of California.

UCRL-9647

UNIVERSITY OF CALIFORNIA
Lawrence Radiation Laboratory
Berkeley, California

Contract No. W-7405-eng-48

MARTENSITE IN CU-12.0% AL ALLOY

G. Thomas and M. C. Huffstutler

April 1961

MARTENSITE IN CU-12.0% AL ALLOY

G. Thomas and M. C. Huffstutler

Inorganic Materials Research Division, Lawrence Radiation Laboratory

University of California, Berkeley 4, California, U. S. A.

ABSTRACT

Thin foils suitable for transmission electron microscopy have been prepared from bulk specimens of Cu - 12.0% Al alloy quenched from 800° C to produce martensite. The martensitic structure consists of long lenticular plates which are twinned on 20-50A scale. The twin planes in the martensite are shown to be $\{10\bar{1}2\}$. There is evidence that this structure is ordered as expected for a transformation from an ordered parent lattice. Experiments using a high temperature stage show that the decomposition of the martensite on tempering can be followed directly, but the martensitic transformation did not recur on cooling.

1. Introduction

The martensitic transformation is usually defined as a phase transformation which occurs by atomic displacements constituting homogenous deformation (shear) and is accompanied by a shape change in the crystal. A detailed review of the crystallographic aspects of martensitic transformations has been given by Bilby and Christian (1955), while the thermodynamic and kinetic approach has been summarized by Kaufman and Cohen (1958). Since the change in shape does not account for the change in crystal structure produced by the transformation, the shear process has been deduced to consist of two components: (1) a macroscopically homogeneous shear producing the shape change, and (2) localized homogeneous shear (Bowles and Mackenzie 1954, 1957; Wechsler et al. 1953; Bilby and Christian, 1955). The second shear produces the required atom movements to form the martensite lattice. The deformation produced by the second shear has been thought to occur either by slip or twinning. As a result of the examination of martensitic structures using the technique of transmission electron microscopy, it has been shown quite clearly that in carbon steels (Kelly and Nutting 1960), and Fe-C, Fe-N, and Fe-Ni alloys (Pitsch 1959 a, b), the martensitic structure is in fact twinned on a scale of 15-500Å. In Pitsch's work, however, since the transformations occurred in very thin foils, the crystallographic features were not typical of those found for transformations in bulk material. The reason for this is the lack of three-dimensional constraint in specimens only ~ 1000Å, so that it is necessary to examine specimens prepared from transformed bulk material. In order to obtain more experimental results

concerning the nature of the second shear (and consequently a more general picture of martensitic transformations), it was decided to investigate non-ferrous martensitic reactions since no electron microscopic work has been reported in this area. Because there is considerable general background data on the isothermal and athermal transformations in the copper-aluminum alloys (e.g., Greninger, 1939, Isaitschew et al., 1938, Tarora, 1949, Haynes, 1955, Hunger and Dienst, 1960), the martensitic β' (hcp) phase of the Cu-Al system was chosen for this work.

1.1 Structures in Cu-12.0% Al Alloy.

Above the eutectoid temperature (565° C), the alloy exists as a random bcc solid solution, designated β. Upon rapid cooling, the eutectoid decomposition is suppressed and at about 530° C an ordered phase, also bcc, designated β_1, is formed after a short delay (during an isothermal transformation). Haynes (1955) has reported that the orientation of β_1 is dictated by that of the prior β, since the transition is not one of the lattice itself but rather a rearrangement of the solvent and solute atoms among the lattice sites. During rapid cooling from above 565° C, the martensitic reaction

$$\beta_1 \rightarrow \beta'$$

starts at approximately 390° C, and transformation proceeds only with continued reduction of temperature, i.e., it is not an isothermal transformation.

Early work done by X-ray techniques on the crystallography of the $\beta_1 \rightarrow \beta'$ transformation (Greninger, 1939; Tarora, 1949) indicated that the β_1 phase is ordered bcc (a_o = 5.82 Å, see Fig. 9). Owing to the limited stability of the β' phase with respect to the equilibrium eutectoid constituents α (fcc) and γ_2 (hcp), accurate determinations of its structure and unit cell dimensions have not been

possible. Isaitchew, et. al, (1938) and Greninger, (1939) showed that the β' martensite is distorted hcp with the transformation following the orientation relationships:

$$(110)\ \beta' \parallel (0001)\ \beta'$$

$$[111]\ \beta' \parallel [10\bar{1}0]\ \beta'$$

However, the unit cell dimensions of the β' have not been established with complete certainty. Hunger and Dienst (1960) using X-ray and electron diffraction techniques give a = 5.16Å, c = 6.35Å with c/a = 1.25, whereas Tarora (1949) gives a = 2.59Å and c = 4.198Å with c/a = 1.62 for Cu-13.5% Al martensite- (in the latter case designated as γ', also having a distorted hcp structure). These discrepancies are possibly due to composition differences, twinning, and confusion in the interpretation of the electron diffraction patterns associated with superlattice reflections. Taking this into consideration, Hunger and Dienst's electron diffraction data can be interpreted (Thomas and Huffstutler, 1961) to give a = 2.62Å (it is not possible to obtain a value for the c-axis dimensions from their electron diffraction patterns since these were all basal-plane reflections). In view of these difficulties, it was found necessary to obtain the a and c axes for the martensitic structure observed in the work reported here.

2. Experimental Procedure

Polycrystalline specimens (~0.004" thick) of high purity Cu-Al alloy, analyzed as 12.03 wt.% Al quenched in iced brine after hot rolling within the β range, were lightly polished with emery paper before electro-thinning. Figure 1 shows optical micrographs of the quenched alloy; the structure is typically martensitic. Thin specimens were prepared using the usual bath

for copper alloys (Swann and Nutting, 1960), namely one part conc. HNO_3 to two parts absolute methanol at -25°C. The resulting foils were examined in a Siemens Elmiskop I and a Hitachi H. U. 10 electron microscope operated at 100KV, and electron diffraction patterns were obtained using the selected-area technique. Indexing of the diffraction patterns and determination of the twinning relationships were facilitated by comparing the electron micrographs with the associated diffraction pattern on the same plate (the diffraction pattern is rotated only about 5° with respect to the micrograph using the Hitachi H. U. 10).

To confirm the findings from electron diffraction, and to obtain the unit cell dimensions, electro-polished specimens were mounted on an XRD-3 X-ray spectrometer to record the high-angle diffraction maximum for filtered Cu K_α radiation.

3. RESULTS

3.1 The Structure of β' Martensite.

Although it is thought that β' martensite is hexagonal close-packed, indexing of the selected-area diffraction patterns could not be done until comparison X-ray and electron diffraction patterns were obtained from the same specimen. The results obtained did not fit those quoted by Hunger and Dienst (1960), who also worked with a similar alloy, possibly for reasons which are discussed elsewhere (Thomas and Huffstutler, 1961). The data were, however, in agreement with those reported by Tarora (1949) for the so-called γ' martensite. It is unlikely therefore, that there is a pronounced structural difference between Tarora's γ' martensite and the β' martensite examined in the present work. The electron diffraction patterns were extremely complicated by the appearance of many extra reflections and because of assymmetry in the basal-plane orientations (the a_1 axes was slightly larger than the a_2 and a_3 axes).

However, the X-ray results gave spacings such that an average value of a = 2.57Å was obtained while the c-axis was unambigiously found to be 4.21Å. Using these values, the electron diffraction patterns could all be indexed consistently; Table 1 shows a summary of data obtained from six different foils.

From these results the c/a ratio for β' martensite was obtained as 1.64 which is close enough to the c/a ratio for magnesium (1.625) to permit the use of a standard (0001) magnesium stereographic projection as the basis for the orientation plots for the determination of the twinning planes in the martensite. (Section 3.3)

3.2 Optical Metallography

As suggested earlier, (Haynes, 1955) the orientation of β_1 (and thus β' within a single grain) will be dominated by that of the prior β because of the constraints imposed by ordered structures. As can be seen in Fig. 1a, in some grains a single planar system of β_1 seems to dominate in producing β', while in Fig. 1b at least two systems are clearly in evidence. The martensite structure can be seen to consist of flat lenticular plates (e.g., Fig. 7a); this shape is produced because of the opposing stress fields surrounding each plate and is exactly analagous to mechanical twinning. Also, the plates, which in cross section resemble needles on this scale, have a central plane, or midrib, where the structure on one side is the mirror image of that on the other, i.e., they are related by simple twin orientations. This was confirmed by noting the extinction angles under polarized light. In martensite produced in this way the stresses produced on opposite sides of the midrib can be cancelled by the opposite total shape deformation. All these effects are typical of martensitic transformations.

3.3 Electron Microscopy

Figures 2-4 are typical examples of the martensitic structure. In Fig. 2 alternate platelets show fine striations of uniform thickness ~ 20Å. These

TABLE I

X-RAY DATA			ELECTRON DIFFRACTION DATA	
d, Å	Intensity	Plane	d (= λL/r), Å	Planes
			4.21	(00.1)
2.24	s	(10.0)	2.22	(10.0)
2.12	m	(00.2)	2.11	(00.2)
2.03	vs	(10.1)	2.05	(10.1)
1.95	s	(10.2)	1.92	(10.2)
1.29	m	(11.0)	1.28	(11.0)
1.08	mw	(10.3)		

vs = strongest s = strong m = medium mw = medium weak

striations occur in parallel directions in every other half-plate but are rotated by 120° about the midrib with respect to each successive half-plate*. The diffraction patterns showed that the plates were oriented with [0001] approximately parallel to the beam with the traces of the striations parallel to $\langle 01\bar{1}0 \rangle$. The long axes of the plates lie parallel to $\langle \bar{1}100 \rangle$. These striations proved to be narrow bands of twinned crystal within each plate; dislocations were not observed in any of the specimens. The contrast from the twins arises solely from the orientation differences between the twinned and untwinned parts of the plate, and, like thin precipitates, are seen to best advantage when the twin plane makes a high angle to the foil surface. Twins are not visible when they lie parallel or nearly parallel to the surface. This would account for the poor definition of the markings in certain orientations (e.g., Figs. 3, 4). In any one plate, if the twins are oriented close to a diffracting position, they appear black in the bright-field image and white in the dark-field image; conversely, the contrast from the untwinned parts will be in reverse of this. Both variations of these contrast conditions were observed. The most conclusive evidence of twinning was obtained from the electron diffraction patterns. Figure 5a is a selected-area electron diffraction pattern of the plate A shown in Fig. 2. This shows a single-crystal pattern of a basal-plane and its twin reflection. The distortion in the basal-plane is quite evident and is typical of this orientation. Indexing of this pattern was consistent with the superposition of a $[01\bar{1}0]$ β' projection onto a [0001] β' projection as shown schematically in Fig. 5b. From this the orientation relationship between the twinned and untwinned parts of the β_1 lattice is:

[0001] matrix parallels $[01\bar{1}0]$ twin

---

* As suspected from optical metallography, the midrib is simply a twin axis parallel to $\langle \bar{1}100 \rangle$.

Almost all the specimens examined were oriented with the basal-plane approximately parallel to the foil surface. Presumably this is due to the preferred orientation arising from the hot rolling used to produce the specimens in initial 0.004" strip form. A trace analysis of micrograph selected-area diffraction pairs for crystals in [0001] orientation does not allow the twin plane to be determined uniquely since the normals to all possible planes making the trace are coincident with the zone axes parallel to the a directions in the crystal. Of the possibilities, the probably twin planes are $\{0\bar{1}12\}$, $\{0\bar{1}11\}$ or $\{0\bar{1}10\}$, with $\{0\bar{1}12\}$ being the most likely for twinning in hcp crystals. Even from the area shown in Fig. 4 (which is also in [0001] orientation) where cross twinning is observed, the traces being parallel to $[\bar{1}101]$ and $[10\bar{1}0]$, a stereographic analysis is ambiguous. However, an orientation was found where the twin plane could be determined; Fig. 6a shows a micrograph and Fig. 6b the corresponding selected area diffraction pattern in orientation $[\bar{1}\bar{4}51]$. Figure 7 shows the stereographic projection of this and the traces of the twin plane and the normals to all possible planes making this trace. This projection (based on a standard magnesium crystal projection) is obtained with a rotation of 83° as shown. It can be seen that the $(0\bar{1}12)$ trace is within 2° of a possible twin plane, while the $(0\bar{1}11)$ and $(0\bar{1}10)$ are 7° and 27° away from this. We infer from this analysis that the twin plane is indeed $\{0\bar{1}12\}$ as expected for hcp structures. It can be seen from Fig. 3 that the twins run through the thickness of the plate, e.g., at A. This shows a martensite plate in $[0\bar{1}11]$ orientation tilted so that the twin packets are observable in projection on the top and side of the plate. The $\underline{(10\bar{1}2)}$ plane makes an angle of 49° 10' with $\underline{(0\bar{1}11)}$ which is consistent with the measured angle of 47° obtained from the trace of the twin plane in Fig. 3.

Considering $(10\bar{1}2)$ mechanical twinning in other hcp crystals such as those of Mg and its alloys (Raynor, 1959) it is known that $[0001]_{twin}$ lies almost

perpendicular to $[0001]_{matrix}$. Thus, if the area diffracting in Fig. 5a included a significant amount of the twinned orientation, one would expect both basal and prism-plane reflections. This is exactly what was found. Judging from the clustering of spots and the slightly imperfect symmetry of the (0001) β' projection, the structure is distinctly distorted from a perfect hexagonal arrangement. The basal-plane traces of the cross-markings in Fig. 4 also suggest the presence of twinning on two conjugate $\{10\bar{1}2\}$ planes.

Examination of the diffraction patterns (e.g., Figs. 5a, 6b) shows that the twin spots are streaked in a direction normal to the twin plane. Measurement of the length of the streaks (allowing for its projection in the plane of the reciprocal lattice) corresponds to a twin thickness of 20-50Å which is consistent with the measurements obtained from the micrographs. All these results confirm that the second shear is accompanied by twinning and not by slip and is in agreement with the results obtained by Pitsch (1959) and Kelly and Nutting (1960) on martensitic structures in ferrous alloys. All the electron diffraction patterns showed extra reflections which could not be indexed in terms of twinned or untwinned diffraction spots. Examples can be seen in Fig. 5a, and 6b. From Fig. 5b it can be seen that in the twin orientation $[01\bar{1}0]$ these extra reflections (closed circles) form a cross-grid pattern in projection on the (0001) untwinned orientation. This suggests the possibility of ordering in the martensite probably as a result of the retention of the order exhibited by the β_1 structure during the transformation; this point will be discussed further later (Section 4.).

3.4 <u>High Temperature Experiments</u>

Some work was done using a high temperature stage in the Hitachi electron microscope. This stage has the facility of bi-axial tilting when using a long

focal length objective pole piece, thus enabling contrast to be maintained during heating. However, there is a disadvantage in that the resolution using this pole piece is reduced to ~50Å. Figures 8a, 8b and 8c show a sequence of decomposition of β' at temperatures 200° C, 350° C, and 500° C after three runs at each temperature. No change in structure was observed at 200° C and the twinned β' crystals were clearly resolvable (Fig. 8a). The first stages in decomposition (Fig. 8b) were accompanied by the breakdown of the martensitic plates into fine needles probably of the α phase. Owing to the lack of resolution, it is not clear whether or not these needles form directly at the twin boundaries; the observations indicate they probably do not. Nucleation was observed along the edges of the β' plates and there were always at least two orientations of needles observed in a single original β' plate. This is unlike the behavior of tempered martensite in carbon steels where carbide particles have been observed to form along twin interfaces (Kelly and Nutting, 1960). Upon further holding, the larger needles grew at the expense of smaller ones. At the higher temperatures (Fig. 8c) the β' is completely decomposed and the foil "breaks up" into a lamellar two-phase structure typical of the $\alpha + \gamma_2$ eutectoid (Cope, 1959). Owing to the reduction in volume associated with the final decomposition of β' a series of holes are left in the foil (Fig. 8c). This effect occurred each time the temperature was raised to 500° C and above. Unfortunately, attempts to "quench in" martensite by switching off the heating current were unsuccessful. When this was done there was no further change in the structure shown in Fig. 8c. Consequently, it has not been possible, so far, to observe directly the $\beta_1 \rightarrow \beta'$ martensitic transformation. However, these experiments show that phase transformations can be observed directly in the electron microscope and confirms earlier work done on Al-Cu alloys (Thomas and Whelan, 1961). Owing to the complex nature

of the electron diffraction patterns, it was not possible to identify the products of β' decomposition. However, using metallographic etching techniques (1% aqueous chromic acid solution) the structures observed in Figs. 8b and 8c could be recognized in the light microscope and confirm the findings of Cope (1959). There was no evidence that in thin foils the martensite transformation is reversible, but this may be a peculiarity of the thin foil itself. Further efforts are being made to investigate the fine details of the martensitic transformation in other alloy systems in an attempt to shed more light on possible dislocation reactions which might accompany the transformation.

4. DISCUSSION

Since it is not possible to retain any of the bcc β_1 phase during transformation, it is not possible to determine the crystallographic features of the $\beta_1 \rightarrow \beta'$ phase change. Thus, in this paper the discussion will be concerned only with the structure of the martensite itself. It is possible to obtain a model of the transformed lattice if the findings of Greninger (1938) and others (e.g., see Bilby and Christian, 1955) are accepted - namely, that the transformation obeys the orientation relationships

$$(110)\ \beta_1 \text{ parallels } (0001)\ \beta'$$

$$[1\bar{1}1]\ \beta_1 \text{ parallels } [11\bar{2}0]\ \beta'$$

and using the result that twinning occurs on $\{10\bar{1}2\}$ β'. Figure 9 shows the structure of the ordered β_1 phase (Cu_3Al after Tarora, 1949) with the unit cell drawn in broken lines. The basal-plane of the β' structure lying on (110) β_1 is outlined in heavy lines. This model of the parent structure is consistent with the observation of double twinning on conjugate $\{10\bar{1}2\}$ planes (Fig. 4) since the basal-planes corresponding to the twinned crystal are related directly to the conjugate $\{110\}$ planes of the β_1 phase. The new lattice

resulting from the transformation (110) $\beta_1 \rightarrow$ (0001) β' drawn out from the model of Fig. 9 is shown schematically in Fig. 10; i.e., if there is no loss in order, which is probably (Kurdjumow, 1939), it can be seen that the martensite lattice consists of an ordered arrangement of only aluminum atoms on every parallel $(0\bar{1}10)$ plane separated by sheets consisting of alternate rows of copper and aluminum atoms. This is compatible with the observations made of the electron diffraction patterns, e.g., Fig. 5a where the extra reflections could correspond to a superlattice structure of the type depicted in Fig. 10. However, owing to the complexity of the electron diffraction patterns, no definite conclusions were obtained to confirm that the atomic arrangements shown in Fig. 10 are a true representation of the β' structure.

Now, if the approximate β' unit cell is drawn within the ordered β_1 lattice (i.e., Fig. 10), the unit cell dimensions calculated from a_o $(\beta_1) = 5.04$Å are:

$$a_1 = 2.91\text{Å},\ a_2 = a_3 = 2.52\text{Å},\ c = 4.1$$

The measured diffraction data for β' give

$$a = 2.57\text{Å},\ c = 4.21\text{Å}$$

Using $(a)_{mean}$ for the β' cell drawn within the β_1 lattice, the volume ratio is

$$\frac{V_{\beta' \text{ in } \beta_1}}{V_{\beta' \text{ in measured}}} = 1.014$$

In other words, the transformation produces only a small contraction of the parent lattice when the martensite is formed so that the atom movements involved in the transformation are also very small. This would suggest that the structure depicted in Fig. 10 is essentially correct, and accounts for the distortion in the basal-plane which was a feature of the selected area diffraction patterns (e.g., Fig. 5a).

The narrowness of the twins suggests that their structure is essentially a bundle of stacking faults, i.e., their formation occurs by the motion of partial dislocations in the twinning planes $\{10\bar{1}2\}$ β'. Since in the fcc α phase in Cu-Al alloys the stacking fault energy has been shown to decrease with increasing aluminum content (Howie and Swann, 1961), the possibility of forming faults in the hexagonal Cu-12% Al alloy is not unexpected. More experiments are necessary to decide whether or not this is true.

5. SUMMARY

In conclusion, the results obtained from this investigation are:

1. As in other martensite structures, the β' Cu-Al martensite consists of thin lenticular plates twinned on a 20-50Å scale. The twinning mechanism for the second shear in martensitic transformations involving a degeneracy in lattice symmetry thus seems to be a general phenomenon.

2. The twin planes in the martensite are probably $\{10\bar{1}2\}$.

3. The transformation $\beta_1 \rightarrow \beta'$ probably retains the same degree of order that existed in the β_1 structure, and the small volume change accompanying the transformation accounts for the distortion in the hcp β' lattice.

4. It is possible to observe directly the tempering of the martensite by means of a hot stage in the electron microscope; the transformation was not observed to be reversible. So far it has not been possible to follow directly the nucleation of martensite by "quenching" the alloy in the microscope hot stage.

ACKNOWLEDGMENTS

The authors wish to thank the U. S. Atomic Energy Commission for financial support of this work. They are grateful for helpful discussions with Mr. J. Mote.

REFERENCES

1. B. A. Bilby and J. W. Christian, 1955, Inst. of Metals, Rep. and Mon. Ser., 18, 121.
2. J. S. Bowles and J. K. Mackenzie, 1954, Acta Met., 2, 129, 138, 224.
3. J. S. Bowles and J. K. Mackenzie, 1957, Acta Met., 5, 137.
4. R. G. Cope, 1959, J. Inst. Metals, 26, 330.
5. A. B. Greninger, 1939, Trans., AIME, 133, 204.
6. R. Haynes, 1955, J. Inst. Metals, 83, 105.
7. A. Howie and P. R. Swann, 1961, Phil. Mag. (in press).
8. J. Hunger and W. Dienst, 1960, Z. fur Metallkunde, 51, 394.
9. I. Isaitschev, E. Kanunski and G. T. Kurdjumow, 1938, Trans., AIME, 128, 361.
9. L. Kaufman and M. Cohen, 1958, Prog. Metal Phys., 7, 165.
10. P. M. Kelly and J. Nutting, 1960, Proc. Roy. Soc., (A), 259, 45.
11. G. T. Kurdjumow, 1939, Trans., AIME, 133, 222.
12. W. Pitsch, 1959, (a) Phil. Mag., 4, 577, (b) J. Inst. Metals, 87, 444.
13. G. V. Raynor, Physical Metallurgy of Magnesium and its Alloys, Pergamon Press, 1959, p. 225.
14. P. R. Swann and J. Nutting, 1960, J. Inst. Metals, 88, 478.
15. I. Tarora, 1949, Nippon Kinzoku Gakkai-Si, 13, 6.
16. G. Thomas and M. C. Huffstutler, Acta Cryst., 1961, (in press).
17. G. Thomas and M. J. Whelan, 1961, Phil. Mag., (in press).
18. M. S. Wechsler, D. S. Lieberman and T. A. Read, 1953, Trans., AIME, 197, 1503.

CAPTIONS TO ILLUSTRATIONS

Fig. 1 (a, b) Optical micrographs showing the microstructure of β' martensite (polarized light). X 300.

Fig. 2 Electron micrograph of β' martensite; thin foil prepared from bulk specimen. Orientation [0001]. Notice the transverse twin markings ~20Å thick and rotated about the mid-rib by 120° in each half of the plate. X 40,000.

Fig. 3 Electron micrograph of martensite plates showing surface relief Orientation $(0\bar{1}11)$ parallel to foil surface. The transverse twinning and surface irregularities are clearly visible. The twin trace makes an angle of 47° with the top surface of the plate. X 80,000.

Fig. 4 Electron micrograph showing possible double twinning, e.g., at A. Orientation approximately [0001]. X 80,000.

Fig. 5 Electron diffraction pattern from β'.

(a) Selected area diffraction pattern from the area A shown in Fig. 2. Notice the distorted hexagonal symmetry (outlined), extra reflections, and streaking of the twin spots.

(b) Schematic interpretation of (a). Here a $(0001)_{\beta'}$ and $(0\bar{1}10)_{\beta'}$ orientation (calculated) are superimposed. If the atom rearrangement were produced by a twinning shear in a single thin crystal, the multiplicity of $\{01\bar{1}0\}$ and $\{10\bar{1}1\}$ relpoints would be minimized, as can be seen in (a).

Fig. 6 Fine structure of β'.

(a) Electron micrograph showing dark-and-light contrast effects from transverse twins in β'. There is apparently a surface tilt in the central region of the band.

CAPTIONS TO ILLUSTRATIONS (cont'd)

(b) Corresponding selected area electron diffraction pattern from (a) showing the trace of the twin plane. Orientation $[\bar{1}\bar{4}51]\ \beta'$.

Fig. 7 Twin-trace analysis based on Fig. 6. The stereographic projection of twin traces from a crystal of $[\bar{1}\bar{4}51]_{\beta'}$ orientation showing that the twin trace is within 2° of that of the $(0\bar{1}12)$ plane.

Fig. 8 Electron micrographs showing structure produced by tempering β' in a hot stage in the electron microscope.

(a) β' after 30 minutes tempering at 200°C. Short times at temperatures below 350°C did not result in decomposition of β'. X 30,000.

(b) β' after 10 minutes at 400°C. Area taken at edge of foil near that shown in (a). This structure is probably α needles in a martensic matrix. X 20,000.

(c) β' after 25 minutes at 400°C. This is similar to the equilibrium eutectoid structure, but notice that the light areas are in fact holes in the foil. X 20,000.

Fig. 9 Schematic representation of the β_1 Cu_3Al structure (after Tarora, 1949) showing the $(0001)_{\beta'}$ (heavy lines) - $(110)_{\beta_1}$ orientation relationship. The unit cell parameter for β_1 is 5.82Å.

Fig. 10 Schematic representation of the hexagonal β' structure drawn out from the lattice of Fig. 9 with no atomic rearrangements. Notice the ordered arrangement of atoms on alternate prism planes, and the asymmetry of the a axes (see also Fig. 9). The unit cell dimensions are $a_1 = 2.91$Å, $a_2 = a_3 = 2.52$Å.

A

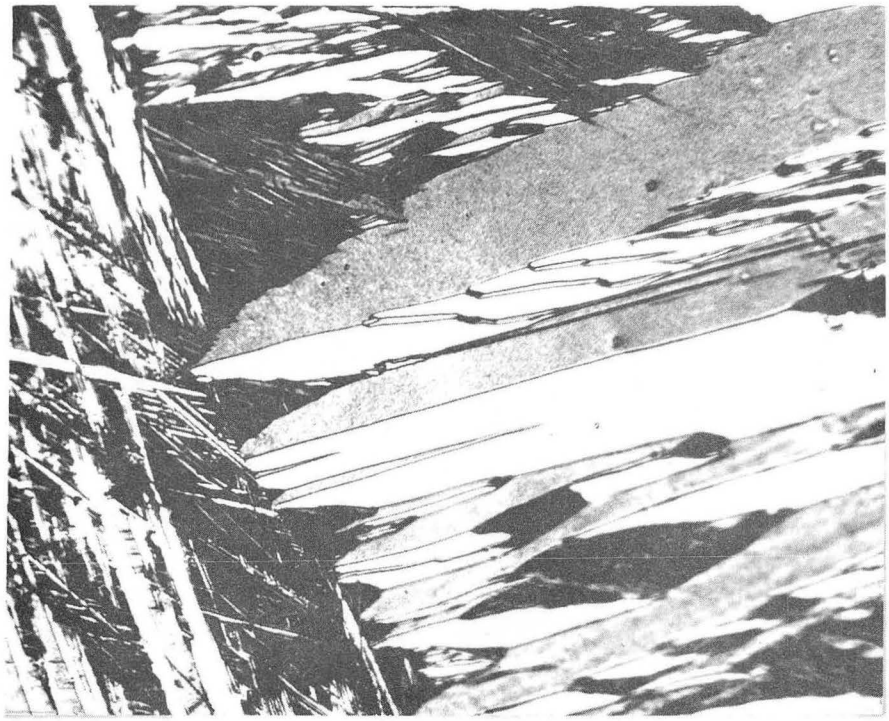

B

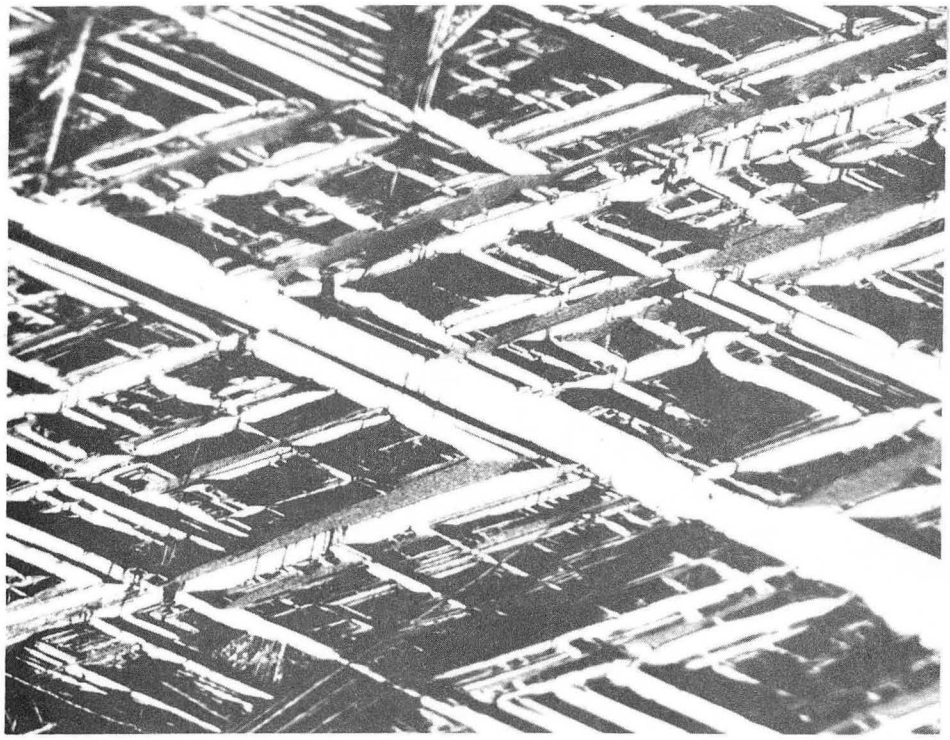

ZN-2788

Fig. 1a and 1b.

ZN-2786

Fig. 2.

ZN-2790

Fig. 3.

ZN-2791

Fig. 4.

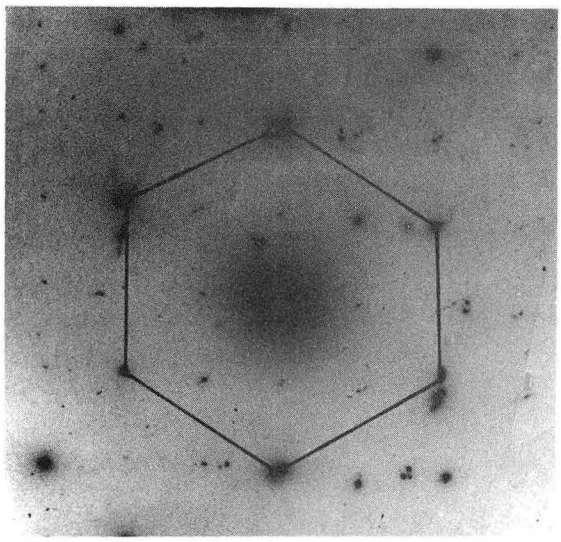

ZN-2785

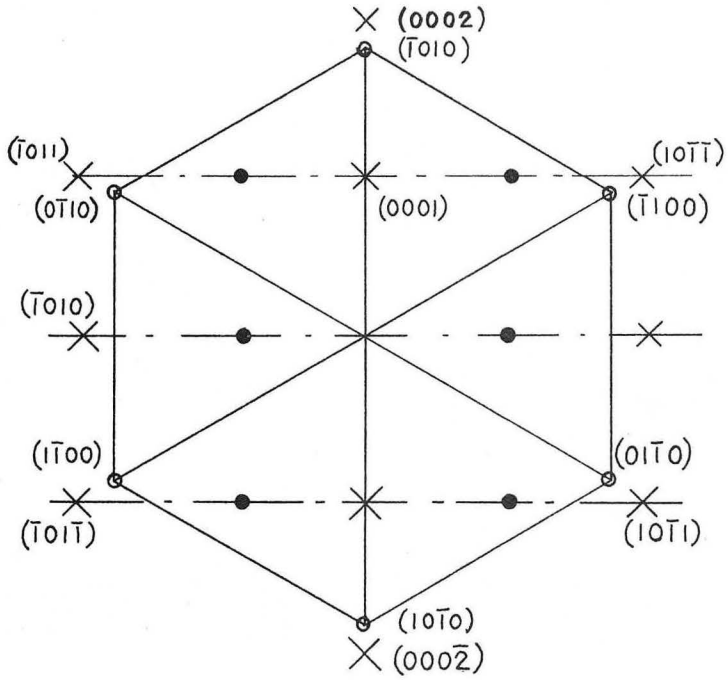

× Twin reflections
o Matrix reflections
● Possible superlattice reflections

MU-22868

Fig 5a and 5b.

A

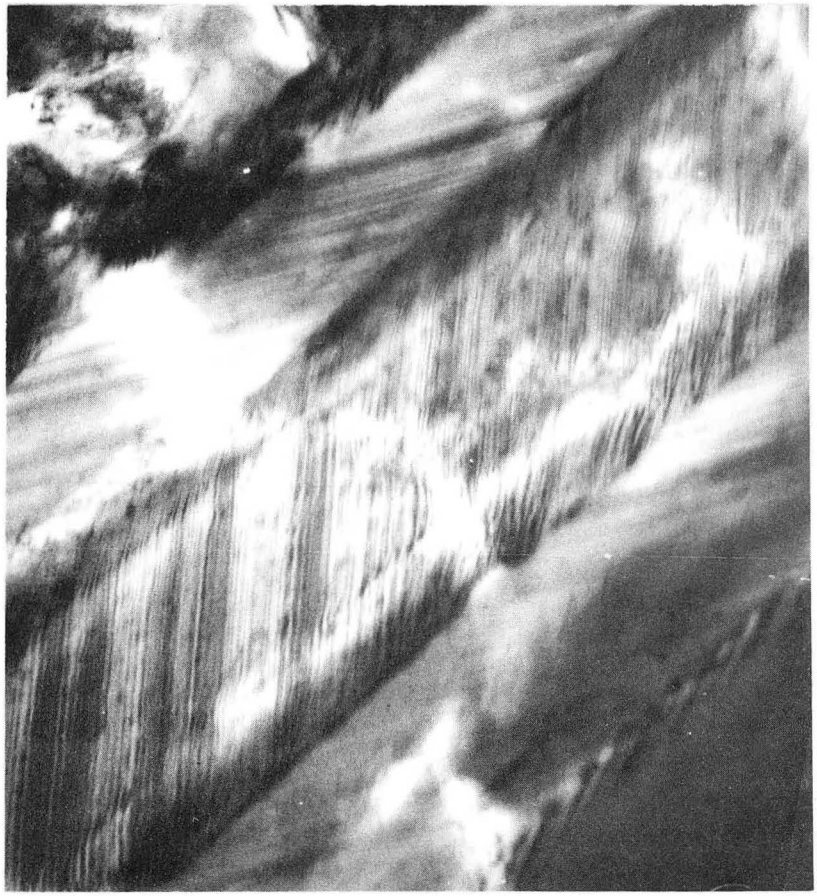

B

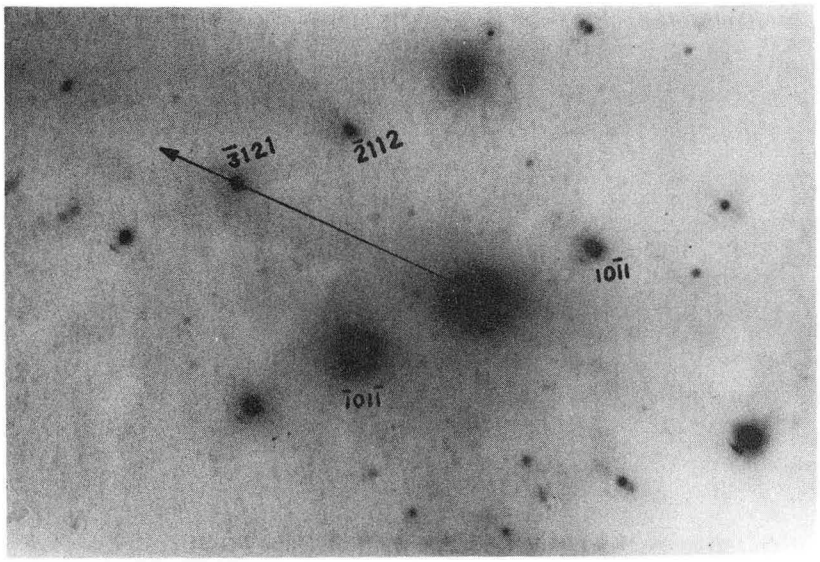

ZN-2789

Fig 6a and 6b.

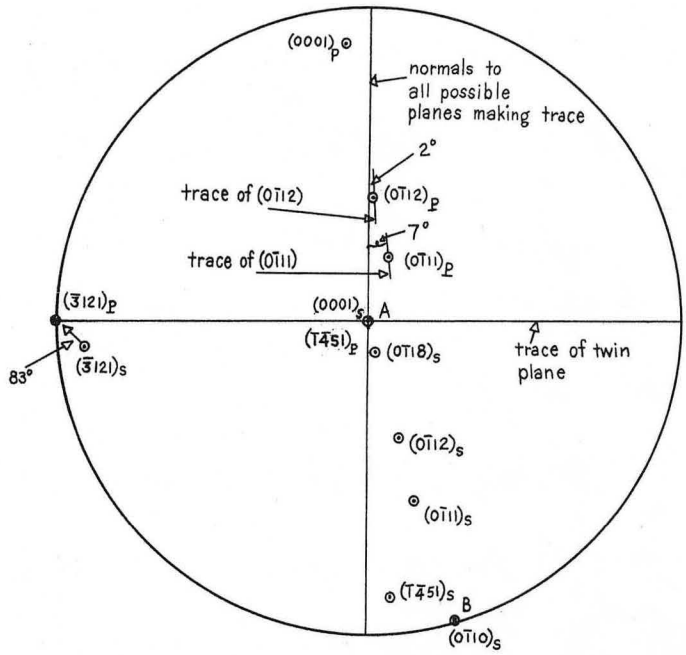

Stereographic projection of [$\bar{1}\bar{4}$51] β' Martensite
Analysis of twin traces shows twin planes are {0$\bar{1}$12}

MU-22871

Fig. 7.

A

B

C

ZN-2787

Fig. 8a, 8b and 8c.

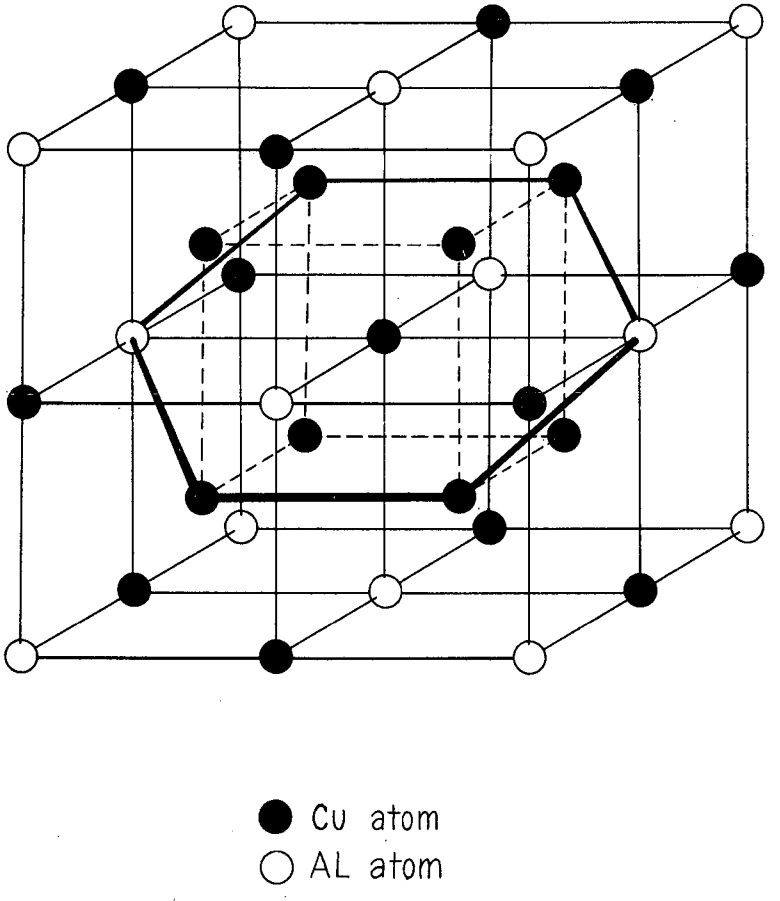

Fig. 9.

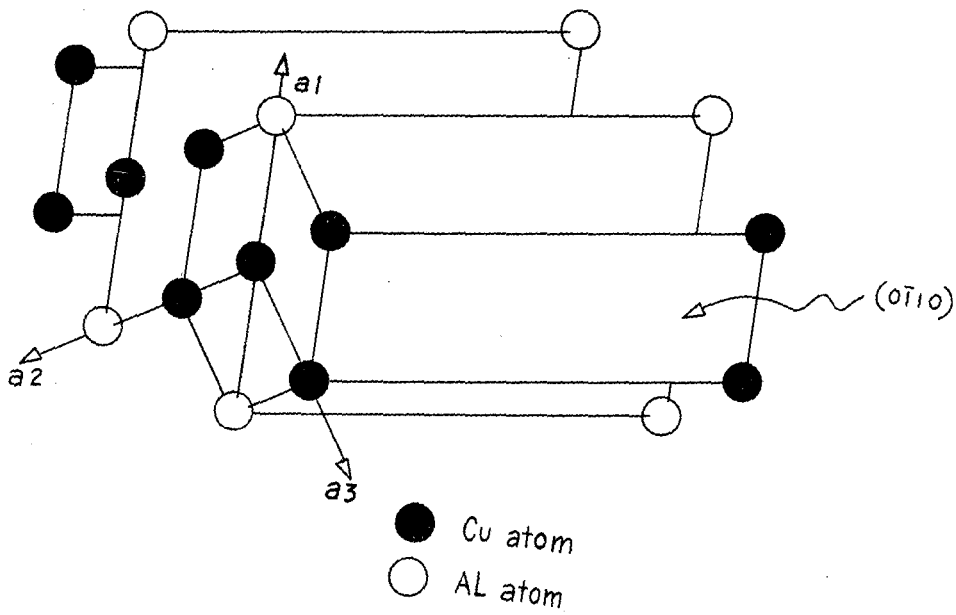

MU-22870

Fig. 10.

LEGAL NOTICE

This report was prepared as an account of Government sponsored work. Neither the United States, nor the Commission, nor any person acting on behalf of the Commission:

A. Makes any warranty or representation, expressed or implied, with respect to the accuracy, completeness, or usefulness of the information contained in this report, or that the use of any information, apparatus, method, or process disclosed in this report may not infringe privately owned rights; or

B. Assumes any liabilities with respect to the use of, or for damages resulting from the use of any information, apparatus, method or process disclosed in this report.

As used in the above, "person acting on behalf of the Commission" includes any employee or contractor of the commission, or employee of such contractor, to the extent that such employee or contractor of the Commission, or employee of such contractor prepares, disseminates, or provides access to, any information pursuant to his employment or contract with the Commission, or his employment with such contractor.